[BIO06] Interaction of isoniazid with *Mycobacterium tuberculosis* enoyl-acyl carrier protein reductase (InhA): from bioinformatics perspective.

Choong Yee Siew, Habibah A Wahab, Pazilah Ibrahim, Amirin Sadikun

School of Pharmaceutical Sciences, Universiti Sains Malaysia, 11800 Minden, Penang, Malaysia.

Introduction

Tuberculosis (TB), caused by *Mycobacterium tuberculosis* is a leading killer that has plagued mankind for centuries. The disease is estimated to infect 8 million and kill 2 - 3 million people each year (Rouse *et al*., 1995; Manca *et al*., 1997). A frequently used drug to treat TB is isonicotinic acid hydrazide (INH/ isoniazid) but unfortunately, INH-resistant *M. tuberculosis* organisms are becoming quite common now. In a recent survey of 35 countries, 12.6 % of *M. tuberculosis* isolates were found to be resistant to at least one drug, including INH (Ahmad & Mustafa, 2001).

Studies strongly implicated an enzymatic step(s) in the elongation of fatty acids, and the biosynthesis of the very long fatty acyl chains of mycolic acids as the site of action of INH (Winder & Collins, 1970; Davidson & Takayama, 1979; Quemard, 1991). The *inhA* gene product, InhA, was proposed involved in the synthesis of fatty acids, presumably the unique mycolic acid components of the outer mycobacterial cell and has been suggested to be the site of action of INH (Banerjee *et al*., 1994; Wang *et al*., 1998; Vilchèze *et al*., 2000).

The deletions and missense mutations within the *katG* gene are common in INH-resistant clinical isolates of *M. tuberculosis* added evidences in support of the role of *katG*-encoded catalase-peroxidase (Stoekle *et al*., 1993; Heym *et al*., 1995). These strongly suggest that INH is a prodrug which requires the *katG* gene product, KatG, to be activated as an antitubercular (Zhang *et al*., 1996; Manca *et al*., 1999; Lei *et al*., 2000). Once metabolized by KatG, the activated INH metabolite reacts with nicotinamide adenine dinucleotide (NAD^+) to form isonicotinic acyl-NADH (INADH), which is the inhibitor of InhA.

Zhang *et al.* (1992) confirmed that the resistance towards INH is related to the loss of KatG catalase activity. Besides *katG* mutations, mutations in several genes such as *inhA*, *ahpC*, *kasA* and *ndh* (Vilchèze *et al*., 2000; Torres et al., 2000) and genomic regions of *M. tuberculosis* are involved in the occurrence of resistance to INH (Piatek *et al*., 2000; Slayden & Barry, 2000). Banerjee *et al*. (1994) have shown that low-level resistance to INH in some mycobacterial strains is associated with mutations in the *inhA* gene. Mutations occurring in both *katG* and *inhA* genes may account up to 80% of all organisms resistant to this critical antituberculosis agent (Morris *et al*., 1995; Musser *et al*., 1996) with the mutations in *katG* account for the majority of INH-resistant clinical isolates (Cynamon *et al*., 1999; Torres *et al*., 2000).

Reports (Rouse et al., 1995; Miesel *et al*., 1998; Rozwarski *et al*., 1998) have shown that some INH resistant tuberculosis isolates had a single base change, from thymine to guanine at nucleotide 280 resulting in a serine to alanine replacement in codon 94 (S94A) in *inhA* gene. Basso *et al.* (1998) have proposed that INH-resistance in this S94A mutation strain is related to the reduced NADH binding affinity for enoyl reductase. This is supported by an X-ray crystallographic study which showed that there is a reduction in the hydrogen bonding network between NADH and InhA enzyme.

Molecular modeling techniques have been used to understand the mechanism of interaction between a protein and a ligand, substrate or inhibitor, at the atomic level. Molecular docking is one of the most widely used methods to predict the binding mechanism of ligand binding. While molecular dynamics simulations is able to give insights into the natural dynamics on different timescales of biomolecules. Here, we report a study utilizing molecular docking and molecular dynamics simulations in our effort to understand the interactions of INH and also to address the mechanism of resistance by *M. tuberculosis* towards it at the atomic level.

Materials and methods

Molecular docking

The atomic coordinates of INH and INH derivatives (Figure 1) were generated using HYPERCHEM program (Hypercube, Inc.). The ligands initial structures of INADH and NADH were taken from Brookhaven Protein Data Bank (PDB) coordinates (the ligands of 1ZID and 1ENZ, respectively). The atomic coordinates of the wild type, WT and the mutant type, MT InhA enzymes were taken from the PDB as well. (The PDB ids for WT and MT InhA enzymes are 1ZID and 1ENZ, respectively.) Polar hydrogen atoms were added with the protonate program package and charges from the AMBER force field were assigned to each atom using the kollua.amber utility of AutoDock version 3.0.

The docking experiments were carried out employing the docking program AutoDock3.0. (Morris *et al*., 1998). The grid maps for each atom type in ligands were calculated using AutoGrid3.0 with 90×90×90 points and a grid point spacing of 0.375Å. The Lamarckian genetic algorithm begins by creating a population of 50 individuals with the maximum number of energy evaluations set to 1500000 and maximum number of generations to 27000. The translational step size was 0.2 Å, and the orientational and torsional step sizes were 5.0° in each case. The probability that a particular "gene" would undergo crossover and mutation was 0.80 and 0.02, respectively. An elitism value of 1 was used which was the number of top individuals that will automatically survive into the next generation. The probability of performing pseudo-Solis and Wets local search on an individual was 0.06. 300 iterations were executed per local search with the termination value of 0.01. The maximum number of consecutive successes or failures before doubling or reducing the local search step size was 4 in both cases. A maximum of 100 docking runs were carried out for each ligand. After multiple docking runs, cluster analysis was carried out. In each docking, results differing by less than 1.5 Å root mean square deviations were grouped into clusters.

Molecular dynamics simulations

All MD simulations presented in this work were performed by using the Amber version 8.0 simulation package (Case *et al*., 2004), the Cornell *et al*. (1995) all atom force field and the parm99.dat parameter set (Cheatham *et al*., 1999) with the TIP3P water model (Jorgensen *et al*., 1983) and primary cut off distance for non-bonded interactions were set to 12.0 Å.

The starting structure of INADH-WT InhA complex was taken from the PDB (PDB ID: 1ZID). While for INADH-S94A MT InhA, the S94A structure was taken from PDB (PDB ID: 1ENZ) and the INADH structure was taken from lowest docked energy in the most populated cluster since the INADH-S94A complex was not posted in PDB. Na^+ ion(s) were added to the systems to ensure explicit net neutralizing counterions. All the systems were immersed in a 10 Å length truncated octahedron box. The crystallographic water molecules in the both WT and MT complex were retained to preserve the core water molecules involved in the specific hydrogen bonding with the protein residues. The INADH, INADH-WT and INADH-S94A system have total of 5655, 27559 and 27957 atoms, respectively.

The system was subsequently energy minimized with steepest descend method for 1000 steps, followed by conjugate gradient for another 1000 steps. For MD simulations, a total 500,000 steps was run with the time step of 2 fs which correspond to 1 ns of MD were performed. All simulation started at 0 K temperature, slowly warmed up and maintained at 300 K using the Berendsen coupling algorithm (Berendsen *et al*., 1984) with 0.5 pico-second (ps) coupling time. Computational time and space were saved where all bonds involving hydrogen atom were constrained and were omitted using SHAKE algorithm (Ryckaert *et al*., 1977). The trajectory for MD simulation was collected and analysed for the last 800 ps of the simulation. Structural fluctuation was analysed using ptraj module in AMBER8.

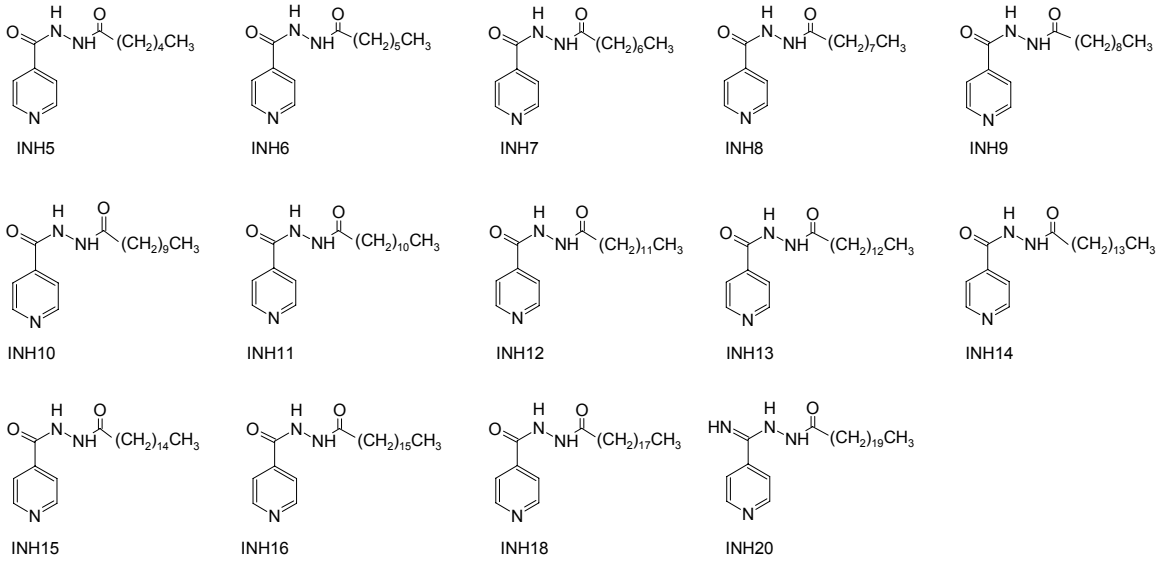

FIGURE 1 The chemical structure of INH derivatives (INH5 to INH16, INH18 and INH20).

Results

Figure 2 shows the superimposition of the WT InhA on the MT InhA enzyme crystallographic structure with the root mean squared deviation, rmsd (of the backbone) of 0.61Å indicating that there is a high structural similarity with minor differences between the WT and the MT enzymes as a result of mutation of serine 94 to alanine. The deviation in structures was found mainly within the region near the mutant site. Upon docking of INA-NADH to the WT InhA, it was found that the ligand docked in almost the same binding mode within an rmsd of 1.054 Å (Figure 3). Docking of NADH on the MT InhA showed an rmsd of 0.982 Å for the lowest free energy of binding structure with the crystal structure (Figure 4). As discussed by Jones and co-workers (1995) and Kramer and co-workers (1999) a value of rmsd less than 2 Å is considered acceptable for docking solutions.

The rmsd between the INADH docked onto the mutant enzyme with the reference structure (crystallographic structures in WT InhA; PDB ID: 1ZID) is 2.519 Å (Figure 3). This indicates that molecular docking is able to distinguish the interaction in the WT and MT InhA. INH was also found to dock within the active site of the WT InhA, forming two hydrogen bonds with the enzyme. In contrast, INADH forms nine hydrogen bonds while NADH forms eight hydrogen bonds with the enzyme. In the MT enzyme, it was found that while the hydrogen bonds formed with INH remains unchanged, there were marked reductions of hydrogen bonds formed in NADH and more so in INADH. A summary of hydrogen bonding interactions of the ligands, INA-NADH, NADH and INH is represented in Table 1 (also Figure 5 and 6).

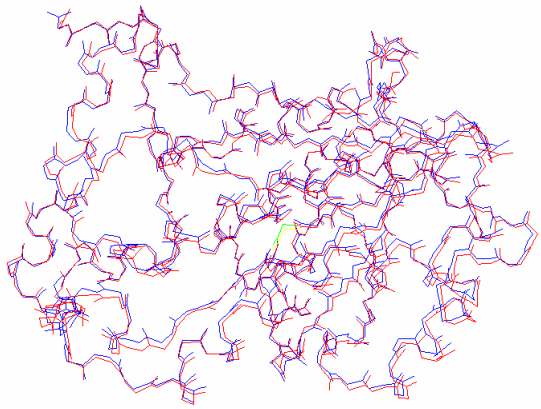

FIGURE 2 The line model of superimposed of WT (blue line; PDB ID: 1ZID) and S94A MT InhA (red line; PDB ID: 1ZID). The WT serine94 is in green line while the MT alanine94 is in yellow line. The backbone root mean square deviation between the two structures is 0.61 Å.

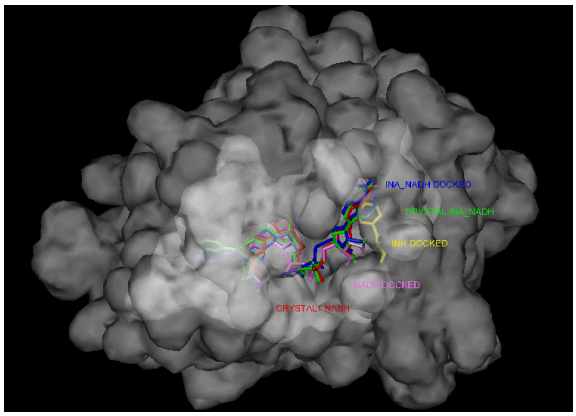

FIGURE 3 Docked conformation of isoniazid (INH; yellow sticks presentation), NADH (pink sticks), isonicotinic acyl-NADH (INADH; blue sticks) and the x-ray crystallographic structure of INA-NADH (PDB ID: 1ZID; green stick) and NADH (PDB ID: 1ENZ; red stick) in the active site (white surface) of WT InhA (grey surface; PDB ID: 1ZID).

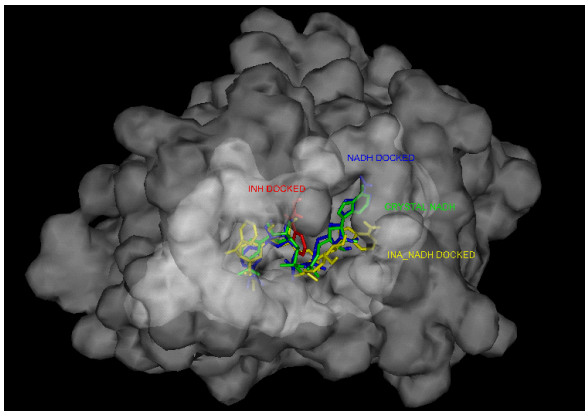

FIGURE 4 Docked conformation of isoniazid (INH; red sticks presentation), NADH (blue sticks), isonicotinic acyl-NADH (INADH; yellow sticks) and the x-ray crystallography structure of NADH (PDB ID: 1ENZ; green sticks) in the active site (white surface) of MT InhA (grey surface; PDB ID: 1ENZ).

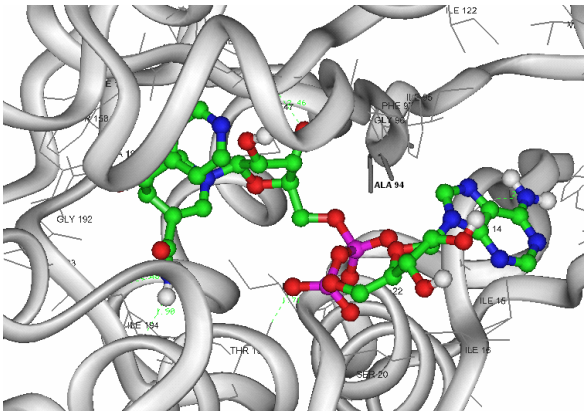

FIGURE 5 Docked conformation of isonicotinic acyl-NADH (INA-NADH; ball and stick) in the active site (grey line) of S94A (grey stick represented alanine94) MT InhA (PDB ID: 1ENZ; ribbon). Green doted line shows the hydrogen bonds between INADH and InhA. Residues within 4Å of INADH are shown.

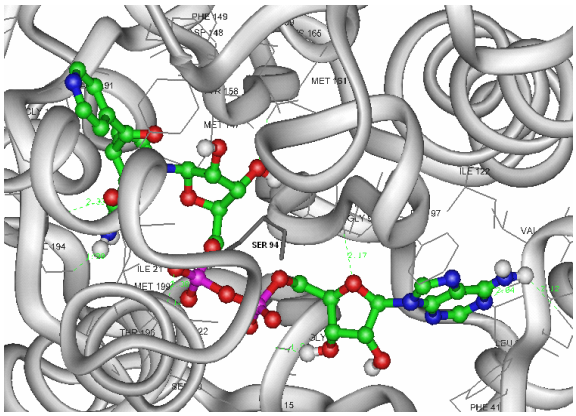

FIGURE 6 Docked conformation of isonicotinic acyl-NADH (INADH; ball and stick) in the active site (grey line; grey stick represented serine94) of WT InhA (PDB ID: 1ZID; ribbon presentation). Green doted line shows the hydrogen bonds between INADH and InhA. Residues within 4Å of INADH are shown.

TABLE 1 Summary of hydrogen bonds, hydrophobic contacts, van der Waals, electrostatic and π-π interactions between isoniazid (INH), NADH and isonicotinic acyl-NADH (INADH) with WT (PDB ID: 1ZID) and S94A MT (PDB ID: 1ENZ) InhA.

	Number of interaction					Docking calculation		
System	H-bond	Hydro-phobic	van der Waals	Electro-static	π-π	Inhibition constant (g/ml)	Free energy (ΔG) (kcal/mol)	RMSD (Å)
WT-INH	2	7	12	12	1	5.67×10^{-5}	-5.79	NA
MT-INH	2	5	9	9	0	1.22×10^{-4}	-5.34	NA
WT-NADH	8	15	26	26	2	8.83×10^{-10}	-12.35	0.94
MT-NADH	6	17	28	28	2	1.95×10^{-9}	-11.88	0.98
WT-INADH	9	16	29	29	4	3.79×10^{-13}	-16.95	1.05
MT-INADH	5	15	27	27	3	4.39×10^{-11}	-14.39	2.52

Table 1 also summarizes the different types of protein-ligand interactions between INH, NADH and INADH and the WT and mutant InhA. The residues within 4.2 Å from the ligand are taken into account for the van der Waals interactions. The same distance is also used for hydrophobic residues which from hydrophobic contact with the ligand following suggestion by Torshin (1999) that the hydrophobic interaction occurs when the distance between two atoms is less than or equal to the sum of their van der Waals radii. INH forms 7 hydrophobic contacts, 12 van der Waals interactions and 12 electrostatics contacts, and NADH has 15 hydrophobic contacts, 26 van der Waals interactions and 26 electrostatic contacts while INADH has same number of hydrophobic contacts with NADH, 29 van der Waals interactions and 29 electrostatic contacts with WT InhA. The pyridine ring of INH with Phe41 in WT InhA also contributed to the π-π interaction. Adenine ring of NADH made π-π interaction with Phe41 and Phe97 in contrast, this ring of INADH only make π-π interaction with Phe41 while its pyridine ring was making this type of interaction with Phe149, Tyr158 and Trp222. In S94A MT InhA, INH made 5 hydrophobic contacts but less van der Waals and electrostatic contacts are observed. The same observation is found for INA-NADH where it forms the same number of hydrophobic contacts, but the number of van der Waals interaction and electrostatic contacts were both reduced to 27. INH did not contribute to the π-π interaction, however in INADH, the pyridine ring was no more making π-π interaction with Trp222. On the other hand, NADH made slightly more hydrophobic contacts, van der Waals interactions and electrostatic contacts in the MT InhA than with the WT InhA but forms the same number of π-π interaction in both the wild and the MT InhA.

It is interesting to note that residues Gly14, Ile15, Ile16, Phe41, Leu53, Asp64, Val65 and Ile95 of the WT InhA interact with INH and are within the NADH binding site of the activated complex (INADH). This clearly shows that INH is actually bound to binding region of the NADH portion of INADH as clearly shown in Figure 3 and 4 which also suggests that this binding region is more important as the ligand binding site.

Table 1 shows the calculated interaction energies for the lowest free energy binding conformations of INADH, NADH and INH. The estimated free energy of binding of INADH to the WT and MT InhA is -16.95 and -14.39 kcal/mol, respectively. In the case of NADH, a slight increased in the free energy of binding was observed (ΔG: WT: -12.35 kcal/mol; MT: -11.88 kcal/mol). Even though INH also binds at the same binding site, it did so with much increased binding free energy (ΔG: WT: -5.79 kcal/mol; MT: -5.34 kcal/mol).

From MD simulation of WT-INADH and MT-INADH, free energy of binding calculations showed the same trend as in docking calculation. (ΔG: WT-INADH: -45.18 kcal/mol; MT-INADH: -43.17 kcal/mol). Average structure from MD simulation of INADH-WT and INADH-MT (Figure 7) show that similar conformation as in docking where the polar phosphate group of INADH shift away from the Ala94 in MT InhA.

The binding conformation of INH derivatives in WT and MT InhA were shown

in Figure 8. Results show that all the INH derivatives were at the same binding site of INADH in both WT and MT InhA. The INH derivatives filled up the active site of WT and MT InhA from the adenine end to the pyridine end of INADH molecule, when going from INH5 (34 atoms) as the smallest size of INH derivative, to INH20 as the largest INH derivative (79 atoms). It is found that the INH derivatives was gradually fill up the active site of WT and MT when the aliphatic chain of the INH derivative getting longer.

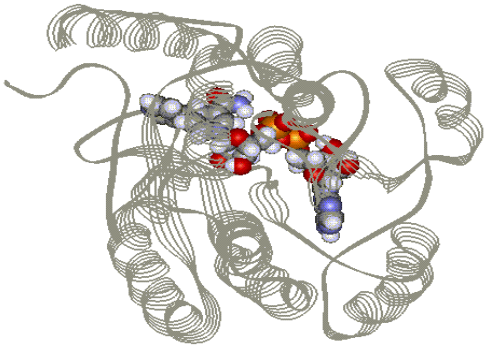

(a)

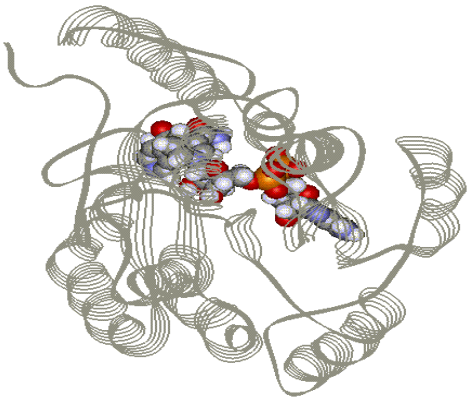

(b)

FIGURE 7 Average structure from MD simulation of a) INADH-WT InhA and b) INADH-MT InhA. INADH in CPK presentation while InhA in line ribbon presentation.

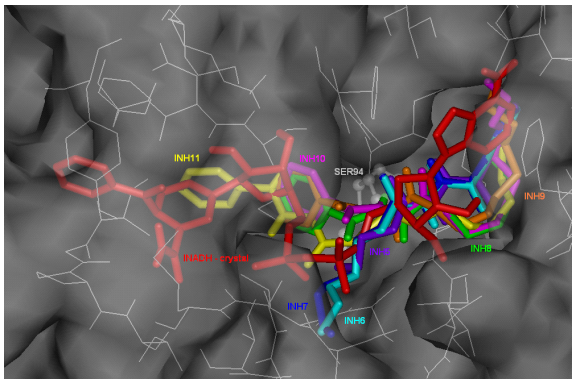

(a)

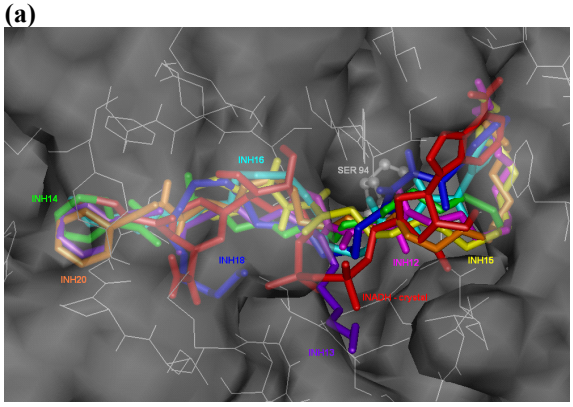

(b)

FIGURE 8 Docked conformation of a) INH5-INH11 and b) INH12-16, INH18 and INH20 in the WT InhA compare with the crystal structure of INADH. surface) of WT InhA (grey surface; PDB ID: 1ZID).

Table 2 shows the estimated free energy of binding (ΔG) in WT and MT InhA. It was observed that the free energy in both WT and MT InhA getting lower when the aliphatic side chain of the INH derivative getting longer. In WT InhA, INH15, INH16 and INH20 were the ligand with the lowest free energy among the INH derivatives. While INH11, INH15 and INH16 were having the lowest free energy in the MT InhA. INH20 docked into WT InhA is the only INH derivatives which has the free energy lower than -10 kcal/mol. INH20 has the inhibition constant (K*i*) value less then 10^{-8} while INH9, INH10, INH12, INH13, INH14, INH15 and INH16 were the INH derivatives which have the K*i* value less then 10^{-7} in WT InhA. In MT InhA, INH11 and INH16 have the K*i* value less then 10^{-8}, while INH7, INH8, INH9, INH10, INH12, INH13, INH14, INH15 and INH20 are the INH derivatives with K*i* value less then 10^{-7} (Table 3.2). From the experimental data (Ibrahim, 1996; Mohamad *et al*., 2004), it was found that INH14, INH16 and INH18 have the lowest minimum

inhibitory concentrations (MIC) of 0.010 µg/ml in H37Rv WT *M. tuberculosis*. MIC value is going lower from ligand with a short aliphatic side chain (INH5) to ligand with longer aliphatic side chain (INH18). Figure 9 shows that the docking results were consistent with the experimental MIC value where the K*i* value is getting lower from INH derivative with a short aliphatic side chain (INH5) to INH derivative with longer aliphatic side chain (INH20).

TABLE 2 Calculated energy of INH derivatives docked into WT and MT InhA.

Ligand - InhA System	Calculated Free Energy (ΔG, kcal/mol)	Inhibition constant, K_i (g/ml)
INH5 - WT	-6.97	7.77×10^{-6}
INH5 - MT	-7.65	2.46×10^{-6}
INH6 - WT	-7.30	4.47×10^{-6}
INH6 - MT	-7.83	1.83×10^{-6}
INH7 - WT	-7.68	2.35×10^{-6}
INH7 - MT	-8.19	9.90×10^{-7}
INH8 - WT	-7.84	1.78×10^{-6}
INH8 - MT	-8.51	5.57×10^{-7}
INH9 - WT	-8.25	9.03×10^{-7}
INH9 - MT	-8.45	6.44×10^{-7}
INH10 - WT	-8.45	6.40×10^{-7}
INH10 - MT	-8.71	4.15×10^{-7}
INH11 - WT	-8.07	1.22×10^{-6}
INH11 - MT	-9.57	9.73×10^{-8}
INH12 - WT	-9.24	1.60×10^{-7}
INH12 - MT	-8.56	5.35×10^{-7}
INH13 - WT	-8.39	7.11×10^{-7}
INH13 - MT	-9.14	1.98×10^{-7}
INH14 - WT	-8.76	3.82×10^{-7}
INH14 - MT	-9.42	1.24×10^{-7}
INH15 - WT	-9.25	1.66×10^{-7}
INH15 - MT	-9.47	1.15×10^{-7}
INH16 - WT	-9.47	1.14×10^{-7}
INH16 - MT	-9.59	9.36×10^{-8}
INH18 - WT	-8.44	6.52×10^{-7}
INH18 - MT	-9.54	1.01×10^{-7}
INH20 - WT	-10.28	2.92×10^{-8}
INH20 - MT	-9.40	1.28×10^{-7}

Discussions

In this study, we attempted to address the resistance mechanism towards INH. Based on the finding that INH must be activated to form INA-NADH by KatG, we hypothesize that in *katG* mutant or deleted *M. tuberculosis*, INH would not be activated to form the INA-NADH complex. Thus, the interactions of the drug and its active metabolite on InhA can be used to explain the resistance phenomena in the organism.

From the present study, there is a clear deviation in the conformation of INADH in S94A MT InhA in compared to its crystal structure conformation in the WT enzyme. From the analysis of the docked conformations, all the hydrogen bonds made are near to the NADH part of the INA-NADH and none were at the isonicotinic acyl (pyridine ring) region of this ligand. The number of hydrogen bonds made by INA-NADH docked to the WT InhA was 9 compared to 5 by INADH in MT InhA. This probably has weakened the binding affinity of INADH towards mutant InhA. Similar observation was made by Chen *et al.* (2001) upon investigation on the binding of NADH to the WT and MT InhA. It is interesting to note that their calculation showed a marked difference between the experiment and the predicted ΔE. They have attributed this to the fact that the optimization/scoring procedure might not properly account factors such as hydrophobic factors.

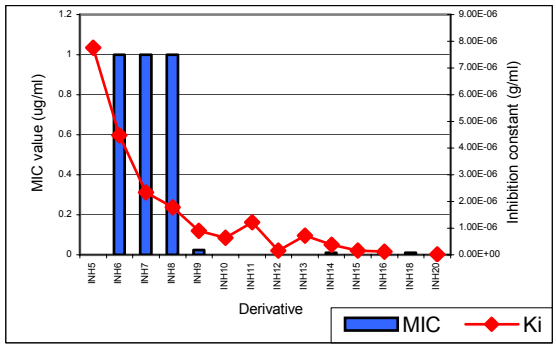

FIGURE 9 Calculated inhibition constant (K_i) value of INH derivatives docked into WT InhA compare with experimental minimum inhibitory concentration (MIC) value of INH derivatives in *M. tuberculosis* H37Rv.

Close inspection of the docked complexes showed that the adenine ring at the NADH part of INA-NADH contributes 75% of the aromatic ring-stacking interaction (π-π interaction). These observations suggest that NADH make an important role for a good binding affinity. The docked conformation also suggests that NADH is a crucial molecule that is needed to bind covalently with INH metabolite before it can act as an antitubercular. These same observations have also been found by Dessen *et al*. (1995) where they suggested that the mechanism of INH may be related to specific interactions

between InhA enzyme and cofactor within the NADH binding site. The phenomenon of the pyridine ring of INADH was sandwiched between Ala191 and Phe149 while adenine ring of INADH was found sandwiched between Val65 and Phe41 has agreed with Denessiouk and Johnson (2000) where these researchers discovered that aromatic ring is often seen sandwiched between hydrophobic residue on one face on the ring and aromatic residue on the opposite face of the ring to strengthen the π-π interaction in INADH. INH is a relatively small molecule (17 atoms) compared with INA-NADH (82 atoms). INADH have more hydrophobic contacts, van der Waals, electrostatic as well as the π-π interactions with InhA in comparison to INH thus explains the lower interaction energies INADH has with InhA than that of INH with the enzyme.

It has been observed by X-ray crystallographic studies that S94A mutant displays a reduced hydrogen bond pattern between NADH and the enzyme. This is consistent with our observation from the docking simulations of WT and MT InhA enzyme. The location of S94A mutation is within the NADH binding region (Figure 5). The serine to alanine mutation at codon 94 in mutant InhA introduces differences in the side chain with the substitution of hydroxyl group in serine to hydrogen in alanine. This has caused the amino acid hydrophobicity property to shift from a polar to non-polar amino acid resulting in the two polar phosphate groups in INADH to drift away from the non-polar Alanine 94 causing the INADH conformation to deviate from the crystal structure with the WT complex. Therefore, it is proposed that the substitution of serine residue by alanine has interferes directly the INADH binding. Further investigation reveals that in the MT enzyme, Asp64 and Val65 are now more than 4Å from INADH and not to be seen within the INADH binding site. Ile21 and Gly94 are also too far away, more than 3Å to be hydrogen bonded with INA-NADH. Furthermore, the hydrogen bond length made by INADH was slightly longer in MT InhA than that in the WT InhA implicating weaker interactions of the ligand in the MT InhA.

It is also worth discussing here that the S94A mutation in InhA even though resulted in deviation docked conformation from the WT enzyme, the calculated ΔG due to the mutation is not as low as should the activated complex could not be formed compare ΔG for INH (unactivated by katG) and INADH (activated complex)]. This implies factors other than the mutation on the InhA are more important to account for the resistance of the mycobacterium towards INH. One such factor could be that InhA is an NADH-dependent enoyl acyl carrier protein reductase. As the co-factor, the presence of NADH is extremely important for the activity of the enzyme and this can be clearly demonstrated from our docking studies where high affinity for binding towards NADH compared to INH is clearly demonstrated. INH can only covalently bound to NADH after it has been metabolized by katG and the binding of NADH only occurs in InhA (Johnsson & Schultz, 1994).

In the present study, we did not consider the involvement of KatG enzyme directly. However, presuming that INH must be metabolized first by KatG enzyme to form the activated INA-NADH that has the inhibitory activity against InhA, then hypothetically, the binding of this compound to InhA must be significantly greater than the parent drug, INH (i.e. the predicted free energy of binding must be more negative or lower Ki value). In fact, the predicted results clearly showed that ΔG for INA-NADH and NADH are much more negative (nearly 3-fold in the case of INA-NADH and 2.1-fold for NADH) compared to INH, indicating that INA-NADH and NADH are highly required for the activity of INH. It can be also postulated that should the activation of INH does not take place either because of mutation or absence of KatG, the INH could still have the activity against the mycobacterium but at the activity much lowered to that if KatG is functional. This result is in agreement with many experimental studies, where most INH resistant strains due to KatG mutation have the MIC of 4.0-5.0 μg/ml in sensitive strains (Lei *et al*., 2000; van Doorn *et al*., 2001).

The lower free energy of binding of INA-NADH and much more lower K_i value of NADH compared to that of INH clearly demonstrate that INA-NADH have better binding affinity of towards InhA and support the experimental observation by Zhang *et al*. (1993), Cynamon *et al*. (1999), Manca, *et al*. (1999), Chouchane *et al*. (2000), and Lei *et al*.

(2000) that INH is a prodrug which needs to be activated by *katG* gene product, the catalase-peroxidase, before it acts as an important antituberculosis (Sarich *et al*., 1998).

Even though it is clear from the argument above that KatG is more responsible to the resistance to INH, InhA is undoubtedly has been shown to be the main site of action for INH. It has a major role in cell wall synthesis and the inhibition of which will eventually lead to *M. tuberculosis* cell death. This should be the basis for its selection as a drug target for the rational design of INH alternatives. This enzyme active site consists of a hydrophobic pocket formed by aromatic and non-polar amino acid residues (Rozwarski *et al*., 1998; Dessen *et al*., 1995). From the binding mode of INADH and the active site of InhA, one can suggest that for drug design, at least at the virtual level, the proposed new structure should not be subjected to the metabolism by KatG but be more hydrophobic so that it can fit into the hydrophobic pockets or it should have a high degree of structural similarity to NADH so that it can competitively bind to the active site with similar affinity to NADH, have some of the key pharmacophoric features of NADH or even being a small molecule which can bind simultaneously with NADH at the binding site.

The differences between the energy from docking and MD simulations is not so surprising because in MD simulations, the water molecules in the binding sites are treated explicitly while the solvent description in docking is limited to the oversimplified atomic solvation parameters (Luzhkov *et al*., 2003).

INH derivatives were the competitive inhibitors in InhA where they were found bind at the same binding site with INADH. Although the INH derivatives bound with both WT and MT InhA in different conformation but they still at the same InhA active site. Since the INADH binding site is the combination of most hydrophobic amino acid therefore it is expected that the INH derivatives, which is consist of aliphatic side chain and is hydrophobic, will fit well and stable in the hydrophobic binding region with INADH (Campbell, 1995; Sewald & Jakubke, 2002). Intermolecular energy is involved in the calculation of free energy in AutoDock (Morris *et al*, 1998), therefore it can be explained that as the aliphatic chain in the INH derivative getting longer, basically there will more van der Waals interaction, electrostatic interaction and hydrophobic contact with InhA binding site and therefore the docked energy is getting lower as the aliphatic chain of INH derivative is getting longer thus increase the binding affinity with InhA. It is found that the number of hydrogen bond, electrostatic interaction, hydrophobic contact, π-π interaction and van der Waals interaction in INH derivatives were more to MT InhA. Therefore it is expected that the estimated free energy of INH derivatives binding were lower than in WT InhA. This trend of improved binding affinity in INH derivatives with longer aliphatic chain has agreed with Rastogi *et al*. (1990) and Mellor *et al.* (2003) that the longer the alkyl chain in a compound, the better anti-microorganism activity the compound will be. The hydrophilic serine to hydrophobic alanine substitution in MT InhA might explained the lower free energy of INH derivatives found in MT InhA where the aliphatic chain of INH derivatives more comfortable in the hydrophobic surrounding (Saint-Joanis *et al*., 1999).

Overall, the INADH still have the favourite free energy and K_i value in both WT and MT InhA as compare with INH derivatives. Therefore, in both WT and MT InhA *M. tuberculosis* INH is still be best solution as is will be hydrolyse into its active form- INADH. In the case of WT InhA with any *katG* mutation where INH cannot be hydrolysed, from the dock results, INH20 will be the best solution to treat mutant *M. tuberculosis* as it was having the lowest free energy and K_i among the INH derivatives. This is agreed with the experimental data where from the longer the alkyl side from the INH, the lower of the MIC value. While in MT InhA with any *katG* mutation, INH11 and INH16 will be the better inhibitor in *M. tuberculosis* INH itself only has a K*i* value of 2.68×10^{-5}. However, although INH derivative with a long alkyl chain show better binding energy and MIC value, but this aliphatic chain might be toxic to the human body. Mellor *et al.* (2003) found that compounds with eight or fewer carbon atoms

in the alkyl chain were non-toxic in tissue culture cells, however, although compounds with alkyl chain length above eight carbon atoms showed better inhibition activity but these compounds also increased the cytotoxicity increase with alkyl chain length. Hence to reduce the cytotoxicity of the INH derivatives, the introduction of an oxygen atom might help where according to Tan *et al*. (1994), the oxygen molecule in the side-chain will reduce the amphiphilicity of the molecule, and also decreases the cellular toxicity and improves the therapeutic index of the compound.

Theoretical calculation results compare with the experimental MIC value from Ibrahim (1996) and Mohamad *et al*. (2004) were found at the same trend. The MIC values the getting lower from INH6 to INH18. However the MIC values given is at the cellular stage where the derivatives might be hydrolysed and form isonicotinic acyl anion or radical by KatG as the amide group of these derivatives is open for KatG attacked and this isonicotinic acyl anion or radical will bind covalently with NADH to form INADH, which is the active inhibitor for InhA. Therefore it can be explained that the MIC for INH6-8 is at higher value. INH9, INH14, INH16 and INH18 were showing very favourable MIC might because of the steric hindrance from by the long alkyl group to protect the amide bond being attack and break by KatG (Shoeb *et al*., 1985; Johnsson & Schultz, 1994; Rozwarski *et al*., 1998), hence these INH derivatives showed a good alternative of INH. A better way of study whether these INH derivatives are better solution to replace INH is by conducting an enzymatic study (Saint-Joanis *et al*., 1999) where only InhA enzyme will be taken into consideration to investigate whether the derivatives is actually inhibit the InhA.

The epidemiologi of tuberculosis has altered due to emergence of HIV infection and the propagation of drug resistant strains and 95% of those new cases and deaths were in developing countries. In short term, cheap, effective and low toxicity chemotherapeutic agents are desperately needed, particularly for the treatment of emerging drug resistant strains (Biava *et al*., 2004) as the lack of priority in the development of novel agents is in part due to a poor financial return on investment available from drugs primarily targeted at a disease which is perceived as a "Third World" problem. Therefore, further understanding of the mode of action of INH derivatives will reveal vital weakness of the tubercle bacillus, which will lead to more effective diagnostics and may be effectively exploited in the production of second generation chemotherapeutics.

Conclusions

Docking results indicated that INH activated to INA-NADH has higher binding affinity towards InhA. The study demonstrated that the activation of INH to INA-NADH not only results in the changes in the way the ligands bind to the target enzyme by making more hydrogen bonds but the activated complex formed made better hydrophobic contact, more van der Waals and electrostatic as well as the aromatic ring stacking interactions which strengthen the binding affinity of INA-NADH compared to the parent compound, INH. The simulation is also able to address the resistance mechanism towards INH in InhA mutant strains of *M. tuberculosis*. The S94A substitution probably causes INH resistance through weak binding of INA-NADH with less hydrogen bond and weaker π-π interactions. Since the binding affinity of INA-NADH and NADH are much greater than INH, it clearly supports that S94A mutation is a low level INH resistance as reported by Banerjee *et al*. (1994). We have also implicitly argued that the presence of KatG is highly necessary so as to convert the INH to INA-NADH the ultimate inhibitor of InhA. The results also suggest that designing new anti-tuberculosis drug that is not subjected to KatG enzyme, or improving the INH structure similar to INA-NADH structure might be a viable approach to overcome INH resistant tuberculosis.

Docking and MD simulations of INADH-InhA showed similarity in the complex conformation. The differences between the energy from docking and MD simulations is because of the difference in the treatment of water molecule.

With the INH derivative molecule size getting bigger, the more interaction were made with the InhA binding site, hence explained the more favourable free energy in a bigger size INH derivatives. However, in the sensitive strain of M. *tuberculosis* (WT InhA),

the INH derivatives have made not much effect towards InhA inhibitions as activated INH still the best inhibitor for InhA. In MT InhA, INADH remains the best inhibitor. However, in the absent of activated INH, INH11 and INH16 remain a better inhibitor compare with un-hydrolyse INH and other INH derivatives. Steric hindrance in long alkyl chain INH derivatives might help to avoid the attack of KatG to break the amide bond. Docking simulation has shown to be able to predict the binding mode of ligand-enzyme as results have also shown that the theoretical calculation and experimental data were correlated with each other. This has also suggested molecular modelling simulation is a viable approach the new drug design. INH derivatives with a longer alkyl chain have higher inhibition activity have agrees with some researches finding (Rastogi *et al*., 1990; Mellor *et al.*, 2003). Overall these data provide further definition of the molecular features of new antituberculosis where the cytotoxicity of these INH derivatives compound with long aliphatic chain can be improved by adding oxygen atom(s). This study has suggested that the designation of new antituberculosis drug or re-design of the INH molecule to improve drug binding affinity a viable approach and might be faster to discover new antituberculosis drug to overcome INH resistance in *katG* or *inhA* gene.

Acknowledgements

The authors wished to thank the Ministry of Science, Technology and Innovation (MOSTI), Malaysia for the National Science Fellowship awarded to Choong Yee Siew. We thank the National Biotechnology Directorate, the Malaysian Ministry of Science, Technology and the Environment for providing the computing resources to our laboratory. This work was supported by USM short-term grant (grant no: 304/PFARMASI/633069).

References

Ahmad, S.; Mustafa, A.S. (2001). Molecular diagnosis of drug-resistant tuberculosis. *Kuwait Med. J*. 33: 120-126.

Banerjee, A., Dubnau, E., Quemard, A., Balasubramanian, V., Um, K.S., Wilson, T., Collins, D., de Lisle, G. and Jacobs, W.R., Jr. (1994). *inhA*, a gene encoding a target for isonaizid and ethionamide in *Mycobacterium tuberculosis*. *Science* 263: 227-230.

Basso, L.A., Zheng, R., Musser, J.M., Jacobs, W.R. Jr. and Blanchard, J.S. (1998). Mechanism of isoniazid resistance in Mycobacterium tuberculosis: an enzymatic characterization of enoyl reductase mutants identified in isoniazid-resistant clinical isolates. *J. Infect. Dis*. 178: 769-775.

Berendsen, H.J.C., Postma, J.P.M., van Gunsteren, W.F., DiNola, A. and Haak, J.R. (1984). Molecular dynamics with coupling to an external bath. *J. Chem. Phys*. 81: 3684-3690.

Biava, M., Porretta, G. C., Deidda, D. Pompei, R., Tafi, A and Manetti, F. (2004). Antimycobacterial compounds. New pyrrole derivatives of BM212. *Bioorg. Med. Chem*.12: 1453-1458.

Case, D.A., Pearlman, D.A., Caldwell, J.W., Cheatham, W.S. III., Ross, W.S., Simmerling, C.L., Darden, T.A., Merz, K.M., Stanton, R.V., Cheng, A.L., Vincent, J.J., Crowley, M., Tsui, V., Radmer, R.J., Duan, Y., Pitera, J., Massova, I., Seibel, G.L., Singh, U.C., Weiner, P.K., and Kollman, P.A. (2004). AMBER 8, University of California, San Francisco.

Campbell, M. K. (1995). *Biochemistry*, 2nd edn. Philadelphia: Saunders College Publishing.

Cheatham, T., Cieplak, P. and Kollman, P.A. (1999). A modeified version of the Cornell *et al*. force field woth improved sugar pucker phases and helical repeat. *J. Biomolec. Struct. Dynam*. 16: 845-862.

Chen, Y. Z., Gu, X. L. and Cao, Z. W. (2001). Can an optimisation/scoring procedure in ligand-protein docking be employed to probe drug-resistant mutations in proteins? *J. Mol. Graphics Modell.* 19: 560-570.

Chouchane, S., Lippai, I. and Magliozzo, R.S. (2000). Catalase-peroxidase (*Mycobacterium tuberculosis* tuberculosis KatG) catalysis and isoniazid activation. *Biochemistry* 39: 9975-9983.

Cornell, W.D., Cieplak, P., Bayly, C.I., Gould. I.R., Mertz, K.M. Jr., Ferguson, D.M., Spellmeyer, D.C., Fox, T., Caldwell, J.W. and Kollman, P.A. (1995). A second generation force filed for the simulation of proteins, nucleic acids, and organic molecules. *J. Am. Chem. Soc*. 117: 5179-5197.

Cynamon, M.H., Zhang, Y., Harpster, T., Cheng, S. and DeStefano, M.S. (1999). High-dose isoniazid therapy for isoniazid-resistant murine *Mycobacterium tuberculosis* infection. *Antimicrob. Agents Chemother*. 43: 2922-2924.

Davidson, L.A. and Takayama, K. (1979). Isoniazid inhibition of the synthesis of monounsaturated fatty acids in *Mycobacterium tuberculosis* H37Ra. *Antimicrob. Agents Chemother*. 16: 104-105.

Denessiouk, K. A. and Johnson, M. S. (2000). When fold is not important: a common structural framework for adenine and AMP binding in 12 unrelated protein families. *Proteins: Struct. Func. Genet*. 38: 310-326.

Dessen, A., Quemard, A., Blanchard, J. S., Jacobs, W. R., Jr. and Sacchettinii, J. C. (1995). Crystal structure and function of the isoniazid target in *Mycobacterium tuberculosis*. *Science* 24: 1638-1641.

Heym, B., Alzari, P.M., Honore, N. and Cole, S.T. (1995). Missence mutations in the catalase-peroxidase gene, *katG*, are associated with isoniazid resistance in *Mycobacterium tuberculosis*. *Mol. Microbiol*. 15: 235-245.

Ibrahim, P. (1996). Studies on the growth cycle, isoniazid susceptibility of *Mycobacterium avium*. PhD thesis. University of Newcastle Upon Tyne.

Hyperchem, version6, 2001, Hypercube, Inc.

Johnsson, K. and Schultz, P. G. (1994). Mechanistic studies of the oxidation of isoniazid by the catalase-peroxidase from *Mycobacterium tuberculosis*. *J. Am. Chem. Soc.* 116: 7425-7426.

Jones, G., Willett, P. and Glen, R. (1995). Molecular recognition of receptor sites using a genetic algorithm with a description of desolvation. *J. Mol. Biol*. 245: 43-53.

Jorgensen, W.L., Chandreskhar, J., Madura, J.D., Imprey, R.W. and Klein, M.L. (1983). Comparison of simple potential functions for simulating liquid water. J. *Chem. Phys*. 79: 926-935.

Kramer, B., Rarey, M. and Lengauer, T. (1999). Evaluation of the FlexX in incremental construction algorithm for the protein-ligand docking. *Proteins: Struct. Func. Genet*. 37: 228-241.

Lei, B., Wei, C-J. and Tu, S-C. (2000). Action mechanism of antituberculosis isoniazid - Activation *Mycobacterium tuberculosis KatG*, isolation, and characterization of *InhA* inhibitor. *J. Bio. Chem.* 275: 2520-2526.

Luzhkov, B. V., Nilsson, J., Århem, P. and Åqvist, J. (2003). Computational modeling of the open-state $K_V1.5$ ion channel block by bupivacaine. *Biochim. Biophys. Acta* 1652: 35-51.

Manca, C., Lyashchenko, K., Colangeli, R. and Gennaro, M.L. (1997). MTC28, a novel 28-kilodalton proline-rich screted antigen specific for the *Mycobacterium tuberculosis* complex. *Infect. Immun*. 65: 4951-4957.

Manca, C., Paul, S., Barry III, C.E., Freedman, V.H. and Kaplan, G. (1999). *Mycobacterium tuberculosis* catalase and peroxidase activities and resistance to oxidative killing in human monocytes *in vitro*. *Infect. Immun*. 67: 74-79.

Mellor, H. R., Platt, F. M., Dwek, R. A., Butters, T. D. (2003). Membrane disruption and cytotoxicity of hydrophobic N-alkylated imino sugars is independent of the inhibition of protein and lipid glycosylation. *Biochem. J.* 374: 307-314.

Miesel, L., Weisbrod, T.R., Marcinkeviciene, J. A., Bittman, R. and Jacobs, W.R. Jr. (1998). NADH dehydrogenase defects confer isoniazid reisistance and conditional lethality in *Mycobacterium smegmatis*. *J. Bacteriol*. 180: 2459-2467.

Mohamad, S. (2002). The effect of isoniazid and its derivatives on *Mycobacterium avium* NCTC 8559. MSc thesis, Universiti Sains Malaysia.

Morris, S., Bai, G.H., Suffys, P., Portillo-Gomez, L. and Rouse, D. (1995). Molecular mechanisms of multiple drug resistance in clinical isolates of *Mycobacterium tuberculosis*. *J. Infect. Dis*. 171: 954-960.

Morris, G.M., Goodsell, D.S., Halliday, R.S., Huey, R., Hart, W.E., Belew, R.K. and Olson, A.J. (1998). Automated docking using a Lamarkian genetic algorithm and an empirical binding free energy function. *J. Comp. Chem*. 19: 1639-1662.

Musser, J.M., Kapur, V., Williams, D.L., Kreiswirth, B.N., van Soolingen, D. and van Embden, J.D.A. (1996). Characterization of catalase-peroxidase gene (katG) and inhA locus in isoniazid-resistant and –susceptible strains of Mycobacterium tuberculosis by automated DNA sequencing: restricted array of mutations associated with drug resistance. *J. Infect. Dis*. 173: 196-202.

Piatek, A.S., Telenti, A., Murray, M.R., El-Hajj, H., Jacobs, W.R. Jr., Kramer, F.R. and Alland, D. (2000). Genotypic analysis of *Mycobacterium tuberculosis* is two distinct populations using molecular beacons: implications for rapid susceptibility testing. *Antimicrob. Agents Chemother*. 44: 103-110.

Quemard, A., Lacave, C. and Laneele, G. (1991). Isoniazid inhibition of mycolic acid synthesis by cell extracts of sensitive and resistant strains of *Mycobacterium aurum*. *Antimicrob. Agents Chemother*. 35: 1035-1039.

Rastogi, N., Goh, K. S. and David, H. L. (1990). Enhancement of drug susceptibility of *Mycobacterium avium* inhibitors of cell envelope synthesis. *Antimicrob. Agents Chemother*. 34: 759-764.

Rozwarski, D.A., Grant, G.A., Barton, D.H.R., Jacobs, W.R. Jr. and Sacchettini, J.C. (1998). Modification of the NADH of the isoniazid target (InhA) from *Mycobacterium tuberculosis*. *Science* 279: 98-101.

Rouse, D.A., Li, Z.M., Bai, G.H. and Morris, S.L. (1995). Characterization of the *katG* and *inhA* genes of isoniazid-resistant clinical isolated of *Mycobacterium tuberculosis*. *Antimicrob. Agents Chemother*. 39: 2472-2477.

Ryckaert, J-P., Ciccotti, G. and Berendsen, H.J.C. (1977). Numerical integration of the Cartesian equation of motion of a system with constraints: molecular dynamics of n-alkanes. *J. Comput. Phys*. 23: 327-341.

Saint-Joanis, B., Souchon, H., Wilming, M., Johnsson, K., Alzari, P. M. and Cole, S. T. (1999). Use of site-directed mutagenesis to probe the structure, function and isoniazid activation of the catalase/peroxidase, KatG, from *Mycobacterium tuberculosis*. *Biochem. J*. 338: 753-760.

Sarich, T. C., Adams, S. T. and Wright, J. M. (1998). The role of $_{L}$-thyroxine and hepatic reductase activity in isoniazid-induced hepatotoxocity in rabbits. *Pharmacological Research*. 38: 199-207.

Sewald, N. and Jakubke, H-D. (2002). *Peptides: Chemistry And Biology*. Weinheim: Wiley-VCH.

Shoeb, H. A., Bowman, B. U., Ottolenghi, A. C. and Merola, A. J. (1985). Peroxidase-mediated oxidation of isoniazid. *Antimicrob. Agents Chemother*. 27: 399-403.

Slayden, R.A. and Barry, III, C.E. (2000). The genetics and biochemistry of isoniazid resistance in *Mycobacterium tuberculosis*. *Microbes Infect*. 2: 659-669.

Stoekle, M.Y., Guan, L., Riegler, N., Weitzman, I., Kreiswirth, B., Kornblum, J., Laraque, F. and Riley, L.W. (1993). Catalase-peroxidase gene sequences in isoniazid-sensitive and -resistant strains of *Mycobacterium tuberculosis* from New York City. *J. Infect. Dis*. 168: 1063-1065.

Tan, A., van den Broek, L., Bolscher, J., Vermaas, D. J., Pastoors, L., van Boeckel, C., and Ploegh, H. (1994). Introduction of oxygen into the alkyl chain of N-decyl-dNM decreases lipophilicity and results in increased

retention of glucose residues on N-linked oligosaccharides. *Glycobiology* 4:141-9.

Torres, M.J., Criado, A., Palomares, J.C. and Aznar, J. (2000). Use of real0time PCR and fluorimetry for rapid detection of rifampin and isoniazid resistance-associated mutations in *Mycobacterium tuberculosis*. *J. Clin Microbiol*. 38: 3194-3199.

Torshin, I. (1999). Molecular surface sequence analysis of several *E. coli* enzymes and implications for existence of casein kinase-2 bacterial predecessor. *Front. Biosci.* 4: D394-407.

van Doorn, H. R., Kuijper, E. J., van der Ende, A., Welten, A. G. A., van Soolingen, D., de Haas, P. E. W., and Dankert, J. (2001). The susceptibility of *Mycobacterium tuberculosis* to isoniazid and the Arg → Leu mutation at codon 463 of katG are not associated. *J. Clin. Microbiol*. 36: 1591-1594.

Vilchèze, C., Morbidoni, H.R., Weisbrod, T.R., Iwamoto, H., Kuo, M., Sacchettini, J.C. and Jacobs, W.R. Jr (2000). Inactivation of the inhA-encoded fatty acid synthase II (FASII) enoyl-acyl carrier protein reductase induces accumulation of the FASI end products and cell lysis of *Mycobacterium smegmatis*. *J. Bacteriol*. 182: 4059-4067.

Wang, J-Y., Burger, R.M. and Drlica, K. (1998). Role of superoxide in catalase-peroxidase-mediated isoniazid action against mycobacteria. *Antimicrob. Agents Chemother*. 42: 709-711.

Winder, F.G. and Collins, P.B. (1970). Inhibition by isoniazid of synthesis of mycolic acids in *Mycobacterium tuberculosis*. *J. Gen. Microbiol.* 63: 41-48.

Zhang, Y., Dhandayuthapani, S. and Deretic, V. (1996). Molecular basis for the exquisite sensitivity of *Mycobacterium tuberculosis* to isoniazid. *Proc. Natl. Acad. Sci. USA*. 93: 13212-13216.

Zhang, Y., Garbe, T. and Young, D. (1993). Transformation with *katG* restores isoniazid-sensitivity in *Mycobacterium tuberculosis* isolated resistant to a range of drug concentration. *Mol. Microbiol*. 8: 521-524.

Zhang, Y., Heym, B., Allen, B., Young, D. and Cole, S. (1992). The catalase-peroxidase gene and isoniazid resistance in Mycobacterium tuberculosis. *Nature (Lond*.). 358: 591-593.